Adaptive Finite Element Methods for Fluid–Structure Interaction and Incompressible Flow

Kristoffer Selim

Thesis submitted for the degree of Philosophiae Doctor
Department of Informatics
Faculty of Mathematics and Natural Sciences
University of Oslo
March 2011

Series of dissertations submitted to the
Faculty of Mathematics and Natural Sciences, University of Oslo
No. 1072

ISSN 1501-7710

Cover: Inger Sandved Anfinsen.
Printed in Norway: AIT Oslo AS.

Produced in co-operation with Unipub.
The thesis is produced by Unipub merely in connection with the
thesis defence. Kindly direct all inquiries regarding the thesis to the copyright
holder or the unit which grants the doctorate.

Adaptive Finite Element Methods for Fluid–Structure Interaction and Incompressible Flow

Kristoffer Selim

Faculty of Mathematics and Natural Sciences
University of Oslo

Abstract

In this thesis, we develop, analyze and implement adaptive finite element methods for fully coupled, time-dependent fluid–structure interaction problems and incompressible flows. The presented adaptive methods are based on *a posteriori* error estimates, where both space discretization and time discretization are adaptively modified based on the solution of an auxiliary linearized dual problem to control the error in a given goal functional of interest. We also include in our analysis the effect of using an inconsistent finite element formulation, such as an operator splitting method, in the computation of the numerical solution. We demonstrate the accuracy and efficiency of the adaptive algorithm with a series of numerical examples.

Keywords: Adaptive finite element method, fluid–structure interaction, *a posteriori* error estimate, dual problem, goal-oriented, incompressible flow, Navier–Stokes, operator splitting method

This thesis consists of an introduction and the following three papers:

Paper I: *An Adaptive Finite Element Method for Fluid–Structure Interaction*

Submitted to journal for publication in 2011.
This paper is co-authored with A. Logg, H. Narayanan and M. G. Larson.

Paper II: *An Adaptive Finite Element Splitting Method for the Incompressible Navier–Stokes Equations*

Submitted to journal for publication in 2011.
This paper is co-authored with A. Logg and M. G. Larson.

Paper III: *An Adaptive Finite Element Solver for Fluid–Structure Interaction Problems*

To appear in *Automated Scientific Computing*, A. Logg, K.-A. Mardal and G. N. Wells (Eds.), Springer, 2011.

The following work is related, but is not included in this thesis:

Paper IV: *Simulating Heart Valve Dynamics in FEniCS*, MekIT'09, B. Skallerud and H. I. Andersson (Eds.), pp. 411-419, Tapir Akademisk Forlag (ISBN: 978-82-519-2421-4), 2009.

Acknowledgments

First and foremost, I wish to express my sincere gratitude to my supervisor Anders Logg for his constant support and availability. His help and encouragement during my studies have been invaluable.

I would like to thank my co-supervisor Harish Narayanan for his support during my studies and, in particular, for his valuable lessons on continuum mechanics. I would also like to thank my co-supervisors Trond Kvamsdal and Nils Svanstedt for all of their valuable comments on this manuscript. Many thanks also go to Mats G. Larson for many fruitful discussions.

Finally, I would like to thank my soulmate Emma Wingstedt for her love and support.

Kristoffer Selim, Oslo, March 2011

Introduction

Contents

1 Introduction

Computer simulation is an important tool in many disciplines of science and engineering. Complex mathematical models are solved in large computer simulations as a complement to experimental techniques and theoretical studies. In order to interpret the results correctly, the quality of the simulations is a key issue. To ensure that a simulation is of high quality, it is crucial that the accuracy of computed solutions can be determined. Moreover, many of the problems that are being simulated in science and in engineering are computationally expensive and computer resources must therefore be used wisely. Ultimately, the solution should be computed with the highest possible accuracy using a given (limited) amount of computing resources.

One such example of a computationally expensive problem is fluid–structure interaction (FSI). This type of problem occurs when a fluid interacts with a solid structure, exerting surface tractions that cause deformation of the structure and, as a consequence, alters the flow of the fluid itself. The occurrence of FSI problems is abundant and this category of problems is of great importance and relevance in many applications. In particular, many problems of interest in biomedical research involve the coupling between a fluid and some kind of solid structure. Blood flow in arteries and the human respiratory system are typical examples. In industrial applications, such as the design of airplanes, pipelines and fishing lures, the analysis of the FSI problem is an important part of the engineering process.

In this thesis, we investigate and design adaptive numerical methods for FSI and fluid flow. We base our investigation on so-called goal-oriented adaptive finite element methods. This provides a general framework for the design of methods that provide error control for a given goal functional that prescribes a physical quantity of interest. In particular, one may use an *a posteriori* error estimate to quantify the error in the computed goal functional and thus determine the accuracy of the computed solution. Based on the *a posteriori* error estimate, one may also design adaptive algorithms for efficient use of computational resources.

1.1 Thesis objectives

The main objectives of this thesis are to:

- derive *a posteriori* error estimates using duality techniques for fully coupled, time-dependent FSI problems and construct a corresponding goal-

oriented adaptive finite element method;

- derive *a posteriori* error estimates using duality techniques for operator splitting schemes for the incompressible Navier–Stokes equations and construct a corresponding goal-oriented adaptive finite element method, including an analysis of the numerical error introduced by the operator splitting;
- develop a user-friendly free/open-source software for goal-oriented adaptive finite element methods for fully coupled, time-dependent FSI problems.

1.2 Main results

Below, we summarize the main results of this thesis, consisting of the contributions presented in Papers I, II and III.

An adaptive finite element method for fluid-structure interaction (Paper I)

In Paper I, we derive a duality-based *a posteriori* error estimate for fully coupled, time-dependent FSI problems. Further, we develop a corresponding goal-oriented adaptive finite element method based on the derived *a posteriori* error estimate. Our methodology relies upon a partitioned primal FSI problem where the three subproblems for the fluid, structure and mesh use separate solvers, making it easy to replace the individual solvers and the governing equations modeling the different subproblems. The primal fluid subproblem is solved in a moving computational domain in the Arbitrary Lagrangian Eulerian (ALE) framework using an operator splitting method. Both the primal structure and mesh subproblems are posed and solved in a stationary reference domain in a Lagrangian framework. By relating the primal fluid subproblem to the stationary reference domain, a corresponding primal problem is formulated in the reference domain, which allows for the derivation of a duality-based *a posteriori* error estimate for the fully coupled, time-dependent FSI problem.

The duality-based *a posteriori* error analysis yields a computable error estimate of the form

$$|\mathcal{M}(e)| \leq E_h + E_k + E_c,$$

where $\mathcal{M}(e)$ is the error in a given goal function $\mathcal{M}$, and E_h, E_k and E_c account for the space discretization error, time discretization error, and *computational*

error, respectively. The computational error E_c measures the effect of the error introduced by using an operator splitting method for the fluid subproblem. The adaptive algorithm adapts the space discretization and time discretization based on the information obtained from E_h and E_k.

Numerical results presented in Paper I demonstrate the accuracy and efficiency of the presented goal-oriented adaptive finite element method. The numerical results also highlight the importance of studying in more detail the effect of the splitting scheme on the size of the computational error E_c.

An adaptive finite element splitting method for the incompressible Navier–Stokes equations (Paper II)

In Paper II, we derive a duality-based *a posteriori* error estimate for an operator splitting scheme for the incompressible Navier–Stokes equations. By comparing the splitting method to a pure Galerkin formulation, the derived *a posteriori* error estimate expresses the error in a goal functional of interest as a sum of contributions from space discretization, time discretization and a term that measures the deviation of the splitting scheme from the pure Galerkin formulation. Based on the error estimate, a goal-oriented adaptive finite element method is developed for control of space and time discretization errors.

Numerical results presented in Paper II demonstrate good performance of the goal-oriented adaptive algorithm. The results indicate that it is possible to combine the simplicity and efficiency of splitting methods for the incompressible Navier–Stokes equations with the powerful framework offered by the finite element method for error analysis and adaptivity.

An adaptive finite element solver for FSI problems (Paper III)

In Paper III, we present a goal-oriented adaptive finite element solver framework for fully coupled, time-dependent FSI problems. The presented solver framework is implemented in a user-friendly Python environment as a part of the collaboratively developed free/open-source project named `CBC.Solve`[1] (released under the GNU GPL). The paper describes the methodology used for solving the partitioned primal FSI problem, including how the different subproblems are solved and implemented. We further discuss strategies for adapting the space and time discretization using the dual-weighted residual method derived in Paper I. The goal-oriented adaptive FSI solver framework is demonstrated

[1] `CBC.solve` is freely available from its source repository at `https://launchpad.net/cbc.solve/` and its only dependency is a working FEniCS installation.

with numerical examples. Code examples are included to demonstrate how our presented methodology is implemented using the finite element software library FEniCS (Logg and Wells, 2010). The presented code illustrates the resemblance between the mathematical notation and the code which is crucial to implement the very complex dual problem for the fully coupled FSI problem. Moreover, we illustrate the flexibility of the solver framework and how one may easily replace or modify the individual solvers for the three subproblems.

1.3 Future work

The presented methodology for adaptive finite element methods applied to fully coupled, time-dependent FSI problems is suited for structures that undergo small to moderate deformation. For large deformations, the mesh smoothing subproblem is a key issue to ensuring a mesh of sufficient quality. Even though the presented method is designed to reduce element distortion for the fluid subproblem by solving an additional mesh smoothing problem, it is not possible to avoid re-meshing for large deformations. To avoid introducing errors when interpolating from an old mesh to a mesh that has been completely or partially re-meshed, a fixed background mesh approach is desirable.

As an approach to handling large deformations, one might consider using the so-called Nitsche's method (Nitsche, 1971). Nitsche's method provides a general approach to weakly imposing interface conditions for various kinds of coupled problems, such as FSI problems. In addition, Nitsche's method may be used to pose interface conditions on overlapping non-matching meshes, which could be used to formulate fixed background mesh methods suitable for FSI problems on complex geometries with large deformations. Since Nitsche's method is formulated as a variational problem, it is also well suited for adapting the space and time discretization using a dual-weighted residual method.

1.4 Outline of the thesis

The purpose of this introductory part of the thesis is to give a general and compact overview of adaptive finite element methods and their application to FSI problems. We start in Section 2 by introducing the finite element method. Next, in Sections 3–4, we go through the basic concepts of duality-based error analysis for finite element methods. In Section 5, we give a brief introduction to FSI problems and discuss their solution in Section 6. Finally, we discuss the application of adaptive finite element methods to FSI problems in Section 7.

2 The finite element method

Engineers all over the world are on a daily basis formulating and solving problems that do not have analytical solutions; instead approximate numerical solutions are necessary. A very successful method for solving a vast diversity of engineering problems is the finite element method. The name was coined by Clough (1960), some years after the method had been introduced for structural engineering applications by Clough and co-workers in Turner et al. (1956). The method was proposed independently by Courant (1943) for the mathematical community without receiving much attention. The mathematical foundation of the finite element method was developed by Galerkin (1915). Galerkin formulated a general method for solving differential equations which is closely related to the variational principles of Leibniz, Euler, Lagrange, Hamilton, Rayleigh and Ritz (Ritz, 1909). Although the majority of users of finite element methods today are engineers in industry, it has a strong mathematical foundation which provides the tools to derive error estimates that can be used in a constructive way to improve the accuracy of approximate numerical solutions.

To obtain a numerical approximation using the finite element method for a given problem, we identify four stages: the *strong problem*, the *weak problem*, the *finite element formulation* and, finally, the *algorithm*. We summarize these stages below for an abstract model problem.

2.1 The strong problem

Differential equations are often formulated in strong form derived from fundamental principles of physics, such as balance of momentum and conservation of mass and energy. We here consider the following strong abstract linear model problem: find the unknown function $u : \Omega \times [0, T] \to \mathbb{R}^n$ $(n = 1, 2, 3)$ such that

$$\dot{u} + Au = f \quad \text{in } \Omega \times (0, T], \tag{1}$$

where $\Omega \subset \mathbb{R}^d$ $(d = 1, 2, 3)$ is an open bounded domain, T a given final time, $\dot{u} = \partial u/\partial t$ denotes the partial time derivative and A denotes a differential operator in space. We also amend (1) with a suitable set of initial and boundary conditions. Equation (1) states that rate of change $\dot{u}+Au$, in space and time, of the unknown u is equal to a given driving force f. The unknown u can represent a wide variety of physical quantities such as a fluid flow, the concentration of a chemical substance over a catalyst bed, or the deformation of a material continuum.

2.2 The weak problem

The starting point of the finite element method is to rewrite the strong problem (1) as a variational or weak problem. The weak form of the problem is obtained by multiplying (1) with a suitable test function v and integrating over the space–time domain. We thus obtain the equation

$$\int_0^T \langle v,\ \dot{u} \rangle \, \mathrm{d}t + \int_0^T \langle v, Au \rangle \, \mathrm{d}t = \int_0^T \langle v,\ f \rangle \, \mathrm{d}t, \tag{2}$$

where $\langle \cdot,\ \cdot \rangle$ denotes the L^2-inner product on Ω. The left-hand side of (2) is typically integrated by parts to move one or two derivatives onto the test function v. By a careful choice of test and trial spaces $\hat{V}$ and V (typically Sobolev spaces), one may phrase the strong problem (1) as the following weak problem: find $u \in V$ such that

$$a(v, u) = L(v) \tag{3}$$

for all $v \in \hat{V}$. This abstract weak problem forms the basis for the mathematical foundation of the finite element method. Under suitable assumptions on the bilinear form $a : \hat{V} \times V \to \mathbb{R}$ and the linear form $L : \hat{V} \to \mathbb{R}$, one may prove existence of the weak solutions; see Debnath and Mikusiński (1999); Kreyszig (1978); Oden and Demkowicz (1996); Brenner and Scott (2008).

We note that we may alternatively write the variational problem (3) in the form

$$0 = a(v, u) - L(v) \equiv r(v) \equiv \int_0^T r^t(v) \, \mathrm{d}t \equiv \int_0^T \langle v,\ \dot{u} \rangle + a^t(v, u) - \langle v,\ f \rangle \, \mathrm{d}t, \tag{4}$$

where $r : \hat{V} \to \mathbb{R}$ is the *residual* and $a^t(v, u) = \langle v,\ Au \rangle$.

2.3 The finite element formulation

To obtain the finite element discretization of the weak problem (3), we seek the solution in a discrete (finite dimensional) subspace $V_{hk} \subset V$ that fulfils the variational problem for all test functions in a discrete test space $\hat{V}_{hk} \subset \hat{V}$: find $u_{hk} \in V_{hk}$ such that

$$a(v, u_{hk}) = L(v) \tag{5}$$

for all $v \in \hat{V}_{hk}$.

The discrete subspaces are constructed by subdividing the domain Ω into a mesh $\mathcal{T} = \{K\}$ of cells K consisting of intervals, triangles and tetrahedra

in one, two and three space dimensions, respectively. Other partitions such as partitions into quadrilaterals or hexahedra are also possible. For the time discretization, we let $0 = t_0 < t_1 < \cdots < t_M = T$ be a partition of $[0, T]$ into time intervals $I_n = (t_{n-1}, t_n]$ of length $k_n = t_n - t_{n-1}$. On each space–time slab $S_n = \mathcal{T} \times I_n$, we make the following *Ansatz* for the finite element solution u_{hk}:

$$u_{hk}(x, t) = \sum_{j=1}^{N} U_j(t)\ \varphi_j(x). \tag{6}$$

Here, $U : [0, T] \to \mathbb{R}^N$ is an unknown vector-valued function that is piecewise polynomial on the partition on the time interval and $\{\varphi\}_{j=1}^N$ is a piecewise polynomial basis on the mesh $\mathcal{T}$.

A fundamental property of the finite element solution is the *Galerkin orthogonality*:

$$a(v, u_{hk} - u) = 0 \tag{7}$$

for all $v \in \hat{V}_{hk}$ which follows by subtracting (3) from (5). The Galerkin orthogonality states that the error $e = u_{hk} - u$ is orthogonal to V_{hk} with respect to the bilinear form a, or that the approximate finite element solution u_{hk} is a projection of the true solution u into V_{hk}.

2.4 The algorithm

To compute a solution of the discrete variational problem (5), we make the assumption that the test functions of $\hat{V}_{hk}$ are piecewise *discontinuous* and polynomial in time. This is the case for the family of cG(q) and dG(q) methods. (Eriksson et al., 1996) We may then take $v(\cdot, t) = 0$ for $t \notin I_n$. It follows that

$$a(v, u) \equiv \int_0^T \langle v,\ \dot{u} \rangle + a^t(v, u)\ \mathrm{d}t = \int_{I_n} \langle v,\ \dot{u} \rangle + a^t(v, u)\ \mathrm{d}t, \tag{8}$$

where now the test function is a polynomial in time on the interval I_n. Similarly, we have $L(v) = \int_{I_n} \langle v,\ f \rangle\ \mathrm{d}t$. By taking v constant on the time interval I_n, it follows that the finite element solution u_{hk} satisfies the variational problem

$$\int_{I_n} \langle v,\ \dot{u}_{hk} \rangle + a^t(v, u_{hk})\ \mathrm{d}t = \int_{I_n} \langle v,\ f \rangle\ \mathrm{d}t \tag{9}$$

for all $v \in \hat{V}_h$ where $\hat{V}_h = \text{span}\,\{\hat{\varphi}_i\}_{i=1}^N$. Inserting the *Ansatz* (6) and noting that $\int_{I_n} \langle v,\ \dot{u}_{hk} \rangle \,\mathrm{d}t = \langle v,\ u_{hk}(\cdot, t_n) - u_{hk}(\cdot, t_{n-1}) \rangle$, we find that

$$M(U^n - U^{n-1}) + \int_{I_n} A_h U \,\mathrm{d}t = \int_{I_n} MF \,\mathrm{d}t, \tag{10}$$

where M is the mass matrix with entries $M_{ij} = \langle \hat{\varphi}_i,\ \varphi_j \rangle$, A_h is the discretized operator (the stiffness matrix) with entries $(A_h)_{ij} = a^t(\hat{\varphi}_i, \varphi_j)$ and F is the vector of nodal basis expansion coefficients for the (projection of the) right-hand side f. For a piecewise linear in time approximation, equation (10) is sufficient to determine the vector of degrees of freedom $U^n = U(t_n)$. Higher order methods require a consideration of higher order moments; that is, one must consider other test functions than those constant in time. In the case of the cG(1) method, we note that the integral $\int_{I_n} A_h U \,\mathrm{d}t$ may be evaluated exactly and find that the solution vector U^n at time t_n can be obtained by solving the linear system

$$\left(M + \frac{k_n}{2} A_h\right) U^n = \left(M - \frac{k_n}{2} A_h\right) U^{n-1} + b^n, \tag{11}$$

where $b^n = \int_{I_n} MF \,\mathrm{d}t$. The cG(1) method is sometimes referred to as the Crank–Nicolson method. We note that extensions may be made to higher order methods and nonlinear problems, in which case one must solve a system of nonlinear equations in each time step.

3 Adaptive finite element methods

Adaptive finite element methods are based on the idea that we want to compute the solution with good accuracy to a minimal computational cost, or, alternatively, compute a solution with as good accuracy as possible to a given computational cost. In many applications, we are interested in finding an accurate solution in terms of a specific target quantity of the solution, a so-called goal functional $\mathcal{M} : V \to \mathbb{R}$. This goal functional is in many situations the main reason for the computation and it expresses a physical quantity of interest. For example, we may want to accurately compute the displacement of a material continuum in a fully coupled fluid–structure interaction problem. To achieve an accurate solution of such a target quantity to a minimal computational cost, we need a reliable computational method that guarantees

$$|\mathcal{M}(u_{hk}) - \mathcal{M}(u)| \leq \text{TOL}, \tag{12}$$

for a given tolerance TOL > 0. The key steps in an adaptive algorithm targeted at achieving (12) using adaptive refinement in space and time are listed below (Algorithm1).

Algorithm 1 Adaptive algorithm

Given a goal functional $\mathcal{M} = \mathcal{M}(u)$ and a tolerance TOL > 0:

0) Select an initial coarse discretization.

1) Compute an error estimate $E \geq |\mathcal{M}(u_{hk}) - \mathcal{M}(u)|$.

2) If $E \leq$ TOL, then stop.

3) Refine the discretization based on the error estimate E.

4) Continue from step 1).

Since u is in general unknown, the important step 1) in Algorithm 1 is far from trivial. To evaluate the error estimate of the goal functional, one may express the error by a so-called duality argument. This technique is explained in the subsequent section.

3.1 Goal-oriented error estimation using duality

In adaptive algorithms for finite element methods, we usually distinguish between two different types of error estimates; *a priori* error estimates and *a posteriori* error estimates. An *a priori* error estimate relates the error to the regularity of the exact global solution u and the resolution h and k in space and time, respectively. The strength of this method is that it provides asymptotic convergence rates for a particular choice of finite element. From a practical point of view, an *a priori* error estimate makes use of information from the exact solution which is not known for many real world applications, such as engineering problems. On the other hand, in an *a posteriori* error estimate, the error is related to the residual of the computed numerical approximation and other computable quantities. Pioneering work on *a posteriori* error analysis of finite element methods was made by Babuška (Babuška and W. C. Rheinboldt, 1978; Kelly et al., 1983; J. P. De S. R. Gago et al., 1983).

The use of duality arguments in adaptive finite element methods was pioneered by Eriksson and Johnson (1991, 1995), followed by the survey paper

Eriksson et al. (1995). In these works, stability properties are derived from continuous dual problems by means of analytic arguments. The duality technique was further developed in Becker and Rannacher (1995, 1996) into the so-called "dual-weighted residual method". In this method, a more general set of goal functionals are analyzed using stability properties derived from the numerical solution of discrete dual problems. The dual-weighted residual method, including mesh adaption based on the discrete dual problem, is summarized in Becker and Rannacher (2001).

Numerous applications of the dual-weighted residual method have followed over the last two decades. Error estimates and adaptive finite element methods derived from these frameworks include ordinary differential equations (Estep and French, 1994; Estep, 1995; Logg, 2004), eigenvalue problems (Heuveline and Rannacher, 2001), systems of reaction–diffusion equations (Estep et al., 2000), plasticity (Rannacher and Suttmeier, 1998), the incompressible Navier–Stokes equations (Becker and Rannacher, 2001; Hoffman, 2004; Becker et al., 2002), reactive flow problems (Sandboge, 1999), the Black–Scholes equation (Foufas, 2008), multiphysics problems (Larson and Bengzon, 2008; Larson and Målqvist, 2007), and free-boundary problems (van der Zee et al., 2010b,c).

In the subsequent sections, we explain the basic concepts of the dual-weighted residual method.

3.2 The dual problem

To analyze the error in a given goal functional $\mathcal{M} : V \to \mathbb{R}$ for the finite element approximation (5) of the weak problem (3), we assume that the goal functional can be expressed as

$$\begin{aligned} \mathcal{M}(u) &\equiv \mathcal{M}_1^T(u(\cdot,T)) + \int_0^T \mathcal{M}_2^t(u)\,\mathrm{d}t \\ &= \langle u(\cdot,T),\ \psi_1^T\rangle + \int_0^T \langle u,\ \psi_2^t\rangle\,\mathrm{d}t, \end{aligned} \tag{13}$$

where $\mathcal{M}_1^T$ is a target functional at the end time $t = T$ and $\mathcal{M}_2^t$ is a target functional integrated over the time interval $t \in [0, T]$. Here, (ψ_1^T, ψ_2^t) denote the Riesz representers of the target functionals.

The error in the goal functional $\mathcal{M}$ may now be represented in terms of the residual $r(v) = a(v, u_h) - L(v)$ of the weak problem (3) and the solution z of an auxiliary dual problem. The (weak) dual problem reads: find $z \in V^*$ such that

$$a^*(v, z) = \mathcal{M}(v), \tag{14}$$

for all $v \in \hat{V}^*$. Here, the pair of dual test and trial spaces are defined as $(\hat{V}^*, V^*) = (V_0, \hat{V})$, where $V_0 = \{v - w : v, w \in V\}$. We note that dual test and trial spaces are obtained by simply swapping the primal test and trial spaces, with the exception that the dual test space is obtained from the primal trial space by subtracting Dirichlet boundary and initial conditions, which is the effect of the construction $v - w$ for $v, w \in V$. Further we note that the definition of the adjoint operator * simply amounts to interchanging the order of the test and trial functions.

We now take a closer look at the abstract dual problem (14) for the specific (abstract) model problem (1). We then have $a(v, u) = \int_0^T \langle v,\ \dot{u} \rangle + a^t(v, u)\ \mathrm{d}t$. The dual problem is thus given by

$$\int_0^T \langle z,\ \dot{v} \rangle + a^t(z, v)\ \mathrm{d}t = \mathcal{M}_1^T(v(\cdot, T)) + \int_0^T \mathcal{M}_2^t(v)\ \mathrm{d}t \tag{15}$$

for all $v \in \hat{V}^*$. This is an initial value problem with initial data ψ_1^T given (weakly) at the final time $t = T$. To see this, we integrate the first term by parts to obtain

$$\begin{aligned} \int_0^T \langle z,\ \dot{v} \rangle\ \mathrm{d}t &= \int_0^T \langle -\dot{z},\ v \rangle\ \mathrm{d}t + \langle z(\cdot, T),\ v(\cdot, T) \rangle - \langle z(\cdot, 0),\ v(\cdot, 0) \rangle \\ &= \int_0^T \langle -\dot{z},\ v \rangle\ \mathrm{d}t + \langle z(\cdot, T),\ v(\cdot, T) \rangle, \end{aligned} \tag{16}$$

since $v \in \hat{V}^* = V_0$ and thus $v(\cdot, 0) = 0$. If now the dual solution z satisfies the initial condition $z(\cdot, T) = \psi_1^T$, where ψ_1^T is the Riesz representer of $\mathcal{M}_1^T$, the boundary terms at $t = T$ cancel and we may write the dual problem in the following form: find $z \in V^*$ with $z(\cdot, T) = \psi_1^T$ such that

$$\int_0^T \langle -\dot{z},\ v \rangle + a^t(z, v)\ \mathrm{d}t = \int_0^T \mathcal{M}_2^t(v)\ \mathrm{d}t \tag{17}$$

for all $v \in \hat{V}^*$ with $v(\cdot, T) = 0$. We note that the Riesz representer of the functional $\mathcal{M}_2^t$ does not have to be computed explicitly since it enters directly as the right-hand side functional in the weak dual problem. It also follows from (17) that the weak dual problem corresponds to the following strong dual problem:

$$\begin{aligned} -\dot{z} + A^* z &= \psi_2^t \qquad \text{in } \Omega \times [0, T), \\ z(\cdot, T) &= \psi_1^T, \end{aligned} \tag{18}$$

together with homogeneous Dirichlet boundary conditions at the Dirichlet boundaries of the primal problem. Here, A^* denotes the adjoint operator of the primal differential operator A.

3.3 Error representation

It now follows directly by taking $v = e = u_{hk} - u$ in (14) that

$$\begin{aligned}\eta &\equiv \mathcal{M}(u_{hk}) - \mathcal{M}(u) = \mathcal{M}(e) \\ &= a^*(e, z) = a(z, e) = a(z, u_{hk}) - a(z, u) = a(z, u_{hk}) - L(z) \\ &\equiv r(z).\end{aligned} \tag{19}$$

In other words, *the error in the goal functional $\mathcal{M}$ is the (weak) residual r of the dual solution z*. We note that for this analysis to be valid, it is necessary that $e \in \hat{V}^*$ so that we may take $v = e$ in (14). This is fulfilled since both u_{hk} and u are members of the primal trial space V. Their difference must therefore be a member of the dual test space $\hat{V}^* = V_0$, provided that the discrete solution u_{hk} satisfies the boundary and initial conditions exactly. (If this is not fulfilled, we may add and subtract the corresponding contributions and include those in the analysis.) We further require that z is a member of the primal test space $\hat{V}$ so that $a(z, u) = L(z)$. This is fulfilled since $z \in V^*$ and $V^* = \hat{V}$. This explains the choice of the dual test and trial spaces.

When analyzing the error of a time-dependent problem, it is useful to isolate the contributions from space and time discretization. We do this by constructing a special interpolant $\pi_{hk} = \pi_k \pi_h : \hat{V} \to \hat{V}_{hk}$ where π_h is a semi-discrete interpolant into the space of piecewise polynomial functions in space at each fixed time t, and where π_k is a semi-discrete interpolant into the space of piecewise polynomial functions in time at each fixed coordinate x. By the Galerkin orthogonality (7), we know that $r(\pi_{hk} z) = 0$. It follows that

$$\begin{aligned}\eta &= r(z) = r(z) - r(\pi_{hk} z) = r(z - \pi_{hk} z) = r(z - \pi_h z + \pi_h z - \pi_{hk} z) \\ &= r(z - \pi_h z) + r(\pi_h z - \pi_{hk} z) \equiv \eta_h + \eta_k,\end{aligned} \tag{20}$$

where η_h represents the error contribution from space discretization and η_k represents the error contribution from time discretization, respectively.

If the computed solution u_{hk} does not satisfy the Galerkin orthogonality (7), we may add and subtract $r(\pi_{hk} z)$ to obtain

$$\eta = r(z - \pi_h z) + r(\pi_h z - \pi_{hk} z) + r(\pi_{hk} z) \equiv \eta_h + \eta_k + \eta_c. \tag{21}$$

The result is an additional contribution to the total error η. We refer to this error as the *computational error*. In Paper I and Paper II, a splitting operator method is used compute the solution. Since the splitting method only partially fulfills the Galerkin orthogonality, we must then account for the additional contribution from E_c.

3.4 Error estimates

3.4.1 Space discretization error estimate $|\eta_h| \leq E_h$

To express the space discretization error η_h as a sum of contributions from the cells of the mesh, we integrate by parts on each cell $K \in \mathcal{T}$ to obtain the error estimate

$$\begin{aligned}
|\eta_h| = |r(z - \pi_h z)| &= \left| \int_0^T r^t(z - \pi_h z)\, \mathrm{d}t \right| \leq \int_0^T |r^t(z - \pi_h z)|\, \mathrm{d}t \\
&\leq \int_0^T \sum_{K \in \mathcal{T}} |\langle z - \pi_h z,\ R_K \rangle_K| + |\langle z - \pi_h z,\ \tfrac{1}{2}[\![R_{\partial K}]\!] \rangle_{\partial K}|\, \mathrm{d}t \\
&= \sum_{K \in \mathcal{T}} \int_0^T |\langle z - \pi_h z,\ R_K \rangle_K| + |\langle z - \pi_h z,\ \tfrac{1}{2}[\![R_{\partial K}]\!] \rangle_{\partial K}|\, \mathrm{d}t \\
&= \sum_{K \in \mathcal{T}} \eta_K \equiv E_h.
\end{aligned} \tag{22}$$

The *error indicators* η_K consist of two residual contributions: the interior cell residual R_K and the facet residual $R_{\partial K}$. The exact form of these contributions varies between different applications and depends on how the weak problem (3) has been obtained from the strong problem (1), but typically R_K is equal to the residual $\dot{u}_{hk} + Au_{hk} - f$ and the boundary term $R_{\partial K}$ represents a flux or a normal stress. Furthermore, $[\![R_{\partial K}]\!]$ denotes the jump of the facet residual over the boundary ∂K of the cell K.

To compute the error estimate E_h, we need to evaluate the error indicators η_K, for which we need access to the dual solution z and its interpolant $\pi_h z$. One may attempt to compute an approximate dual solution z_{hk} by solving the following discrete dual problem: find $z_{hk} \in V_{hk}^* \subset V^*$ such that

$$a^*(v, z_{hk}) = \mathcal{M}(v) \tag{23}$$

for all $v \in \hat{V}_{hk}^* \subset \hat{V}^*$. However, by the Galerkin orthogonality (7), it follows that $r(z_{hk}) = 0$ if $V_{hk}^* = \hat{V}_{hk}$. The error representation (19) thus evaluates to zero

for the discrete dual solution. Furthermore, $\pi_h z_{hk} = z_{hk}$ so the error indicators η_K and thus the error estimate E_h also evaluate to zero if we make the approximation $z \approx z_{hk}$. A common way to overcome this problem is to compute the discrete dual solution in a richer space, say using higher degree polynomials. For a sufficiently smooth dual solution, a higher order method will result in a more accurate dual solution and thus a sharper error estimate. However, in particular for linear problems, the computational cost of solving the dual problem is then significantly higher than the cost of solving the primal problem. To avoid solving the discrete dual solution on a richer space, the discrete dual solution z_{hk} can be computed on the same mesh and using the same polynomial degree as the primal problem, if combined with a recovery/extrapolation procedure. In Rognes and Logg (2010), a simple procedure is presented where one may obtain an enhanced version $\mathcal{E}z_{hk}$ by local extrapolation on patches. We thus replace z by the extrapolated discrete solution and make the approximation

$$z - \pi_h z \approx \mathcal{E}z_{hk} - \pi_h \mathcal{E}z_{hk} \approx \mathcal{E}z_{hk} - z_{hk}. \tag{24}$$

A similar approach is described in Bangerth and Rannacher (2003) for quadrilateral meshes.

3.4.2 Time discretization error estimate $|\eta_k| \leq E_k$

To express the time discretization error η_k as a sum of contributions from each time interval, we write

$$\begin{aligned} |\eta_k| = |r(\pi_h z - \pi_{hk} z)| &= \left| \int_0^T r^t(\pi_h z - \pi_{hk} z)\, \mathrm{d}t \right| \leq \int_0^T |r^t(\pi_h z - \pi_{hk} z)|\, \mathrm{d}t \\ &\leq \sum_{n=1}^{M} \int_{I_n} |r^t(\pi_h z - \pi_{hk} z)|\, \mathrm{d}t \equiv E_k. \end{aligned} \tag{25}$$

In (Logg, 2003), it was noted that the residual r^t behaves like a Legendre polynomial on each time interval I_n under the assumption that the right-hand side f is a piecewise polynomial of the same degree as used to approximate the solution. It follows that the cG(1) residual is zero at the midpoint and takes its maximum (and minimum) values at the endpoints of each interval. We now make the assumption that the interpolant π_k interpolates at the midpoint of each interval to obtain the following approximate estimate based on the computed discrete

dual solution z_{hk}:

$$\begin{aligned} E_k &\leq \sum_{n=1}^{M} k_n |r^t(z_{hk}(\cdot, t_n)) - r^t((z_{hk}(\cdot, t_{n-1}) + z_{hk}(\cdot, t_n))/2)| \\ &= \frac{1}{2} \sum_{n=1}^{M} k_n |r^t(z_{hk}(\cdot, t_n)) - r^t(z_{hk}(\cdot, t_{n-1}))|. \end{aligned} \tag{26}$$

One may similarly construct a suitable interpolant for higher order methods; see (Logg, 2003) for a discussion. We note that the above expression corresponds to using an interpolation estimate with interpolation constant $C = 0.5$ and a finite difference approximation of the time derivative of r^t.

The above estimate E_k is useful as an estimate of the time discretization error η_k. However, it involves the dual solution as a local weight which is impractical in adaptive time step control. In particular, when the adaptive time steps are determined as part of a time-stepping process on a refined mesh, the dual solution has typically been computed on a previous (coarser) mesh and the weights are therefore not directly accessible on the new mesh. For this reason, we derive an upper bound for E_k where the local-in-time dual weights are replaced by a global stability factor. We find that

$$\begin{aligned} E_k &= \int_0^T |r^t(\pi_h z - \pi_{hk} z)| \, \mathrm{d}t = \int_0^T |\langle \pi_h z - \pi_{hk} z, \ R^t \rangle| \, \mathrm{d}t \\ &\leq \int_0^T \|\pi_h z - \pi_{hk} z\| \, \|R^t\| \, \mathrm{d}t \\ &\leq \max_{[0,T]} \{k_n(t) \|R^t\|\} \int_0^T k_n^{-1} \|\pi_h z - \pi_{hk} z\| \, \mathrm{d}t \\ &= S(T) \max_{[0,T]} \{k_n(t) \|R^t\|\} \\ &\equiv \bar{E}_k, \end{aligned} \tag{27}$$

where R^t denotes the Riesz representer of r^t and $S(T) = \int_0^T k_n^{-1} \|\pi_h z - \pi_{hk} z\| \, \mathrm{d}t$ is a stability factor.

3.5 Adaptivity

If it is found that the computed solution u_{hk} does not satisfy the requirement $|\eta| \leq \mathrm{TOL}$, an algorithm is needed to improve the accuracy of the approximate

finite element solution. To reduce the size of the space discretization error η_h, there are essentially three strategies to improve the finite element solution: h-refinement (decreasing the local mesh size), p-refinement (increasing the local polynomial degree) and hp-refinement (a combination of h- and p-refinement). In this thesis, we focus on h-refinement based on the size of the local error indicators η_K.

A number of different algorithms have been proposed for how the cells of the mesh should be marked for refinement based on the size of the local error indicators. An effective marking strategy is so-called Dörfler marking (Dörfler, 1996) in which a large enough subset $\mathcal{T}'$ of all cells (sorted by decreasing indicators) are marked for refinement such that the sum of the corresponding indicators constitute a given fraction α of the total error estimate; that is $\sum_{K\in\mathcal{T}'} \eta_K \geq \alpha E_h$. Another option is to use fixed fraction marking in which a given fixed fraction α of all cells are marked for refinement, again based on a sorting of all cells by the size of their error indicators. Typical values of the parameter α range between 0.1 and 0.5. In Paper I, we compare the two different marking strategies and study the effect of varying the parameter α.

In our work, we have chosen (for simplicity) to keep the mesh constant over the interval $[0, T]$ in each adaptive iteration, as described in Algorithm 1. Each adaptive iteration consists of a solution of the primal problem, the dual problem, evaluation of error estimates and adaptive mesh refinement, as illustrated in Figure 1. The adaptive time steps are determined as part of the time-stepping process; at the end of each time step, the size of the next time step is determined. We emphasize the difference between the refinements in space and time; the mesh remains fixed throughout the time interval and the step size changes in each time step. For a detailed discussion on the time step selection process based on (27), see Logg (2003), Paper I and Paper II.

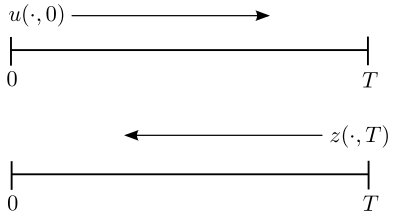

Figure 1: Each adaptive iteration consists of a full solution of the primal problem forward in time, followed by a solution of the dual problem backward in time.

3.6 Extensions to nonlinear problems

We note that if the differential operator A in (1) is nonlinear, then the corresponding weak form is nonlinear. We may again form a corresponding weak primal problem by multiplying the strong problem by a test function v. The weak primal problem then reads: find $u \in V$ such that

$$a(v; u) = L(v) \tag{28}$$

for all $v \in \hat{V}$. We use the notation that the form a is linear in all arguments preceding the semi-colon. Let now $a'(v, \delta u; u) \equiv \frac{\partial a(v;u)}{\partial u}\delta u$ denote the Fréchet derivative of $a(v; u)$ with respect to its second argument. Furthermore, let $\overline{a'}(\cdot, \cdot)$ denote the linearized form averaged over the discrete solution u_{hk} and the exact solution u of the weak primal problem (28); that is

$$\overline{a'}(\cdot, \cdot) = \int_0^1 a'(\cdot, \cdot; su_{hk} + (1 - s)u)\, \mathrm{d}s. \tag{29}$$

The weak dual problem then reads: find $z \in V^*$ such that

$$\overline{a'}^*(v, z) = \mathcal{M}(v) \tag{30}$$

for all $v \in \hat{V}^*$. A similar linearization may be performed to handle any nonlinearities in the goal function $\mathcal{M}$.

To obtain an error representation for the nonlinear problem (28), we note that by the chain rule, the averaged linearized form $\overline{a'}(\cdot,\cdot)$ satisfies

$$\begin{aligned}\overline{a'}(v,e) &\equiv \int_0^1 a'(v,e;su_{hk}+(1-s)u)\,\mathrm{d}s \\ &= \int_0^1 \frac{\mathrm{d}}{\mathrm{d}s}a(v;su_{hk}+(1-s)u)\,\mathrm{d}s \\ &= a(v;u_{hk})-a(v;u) = a(v;u_{hk})-L(v) \\ &= r(v).\end{aligned} \tag{31}$$

It follows that

$$\mathcal{M}(u^{hk})-\mathcal{M}(u) = \overline{a'}^*(e,z) = \overline{a'}(z,e) = r(z). \tag{32}$$

We thus recover the error representation (19). It should be noted that the linearized dual problem depends on the computed discrete solution u_{hk} as well as the unknown exact solution u. In practice, we replace $\overline{a'}^*(v,z)$ by $a'^*(v,z;u_{hk})$; that is, we make the approximation $u_{hk}\approx u$ in the solution of the dual problem.

From a practical point of view, a nonlinear problem requires the solution of the primal problem to be stored on the entire time interval $[0,T]$, since the solution of the linearized dual problem depends on u_{hk}. In each dual time step, one must thus access the solution of the primal problem at the current time before the adjoint linearized operator can be evaluated.

4 Coupled systems of nonlinear time-dependent problems

In this section, we extend the error analysis to time-dependent coupled problems consisting of $m\geq 2$ equations. We do this in preparation for our study of the fully coupled fluid–structure interaction problem. We start by stating the strong form of the model problem for a fully coupled system of nonlinear time-dependent problems. The problem reads: find $u=(u_1,u_1,\ldots,u_m)$ such that

$$\dot{u}_i + A_i(u) = f_i, \quad i=1,2,\ldots,m, \tag{33}$$

together with suitable initial and boundary conditions. The coupled system (33) thus consists of m equations where the couplings between the equations are given by the nonlinear operators $A_i(u)$ for $i=1,2,\ldots,m$. To rewrite the system in

weak form, we construct the total variational problem by summing the weak forms for each individual equation for $i = 1, 2, \ldots, m$. The weak problem reads: find $u = (u_1, u_2, \ldots, u_m) \in V$ such that

$$a_i(v_i; u) = L_i(v_i), \tag{34}$$

where the repeated index i implies summation over $i = 1, 2, \ldots, m$. The test and trial spaces are defined as the following product spaces:

$$\begin{aligned} \hat{V} &= \hat{V}_1 \times \hat{V}_2 \times \cdots \times \hat{V}_m, \\ V &= V_1 \times V_2 \times \cdots \times V_m. \end{aligned} \tag{35}$$

The discrete finite element formulation now follows as before: find $u_{hk} \in V_{hk} \subset V$ such that

$$a_i(v_i; u_{hk}) = L_i(v_i) \tag{36}$$

for all $v \in \hat{V}_{hk} \subset \hat{V}$. Problem (36) can be solved in several ways depending of the characteristics of each individual subproblem.

To obtain the linearized dual problem, we linearize in each component of u. Adopting the notation from Section 3.6, we write

$$a'_{ij}(\cdot, \delta u_j; u) = \frac{\partial a_i(\cdot; u)}{\partial u_j} \delta u_j. \tag{37}$$

With the linearization so defined, we can now introduce the linearized dual problem for the model problem (33): find $z \in V^*$ such that

$$\overline{a'}^*_{ji}(v_i, z_j) = \mathcal{M}_i(v_i), \tag{38}$$

for all $v \in \hat{V}^*$. Here, $\mathcal{M}_i$ denotes a goal functional of interest for subproblem i. The total goal functional is the sum of the goal functionals for the subproblems. We also note the double adjoint in the form of a system-level transpose (subscripts $_{ji}$) and the block-level adjoint *.

Letting $v_i = e_i$ in (38), we obtain the error representation

$$\begin{aligned} \mathcal{M}(u_{hk}) - \mathcal{M}(u) &= \overline{a'}^*_{ji}(e_i, z_j) = \overline{a'}_{ji}(z_j, e_i) = \overline{a'}_{ij}(z_i, e_j) \\ &= a_i(z_i, u_{hk}) - L_i(z_i) = r_i(z_i), \end{aligned} \tag{39}$$

We thus recover the same error representation as in (19).

We notice that the adjoint operation has a special meaning for a coupled system expressed as a sum of variational problems compared to a single variational

problem. We may view the left-hand side of (38) on block form containing the linearized variational problems as blocks. The dual problem is obtained by first taking the transpose of the block-system and then taking the adjoint of each block operator.

5 Fluid–structure interaction

In its most simple form, fluid–structure interaction (FSI) occurs when a fluid interacts with a solid structure, exerting surface tractions that cause deformation of the structure and, thus, alters the fluid flow. By definition, an FSI problem is a true multiphysics problem where the different physics of the fluid and the solid mutually exchange data that define the fully coupled FSI problem. This category of multiphysics problems is of great importance and of great relevance in both industrial applications as well as in many areas of research, such as biomedicine. The design of airbags, bridges and airplanes are typical examples of industrial applications where the analysis of an FSI problem is an important part of the engineering process. In biomedical research, a vast number of problems consist of the coupling between a fluid and a solid. As an example, blood flow in arteries and the resulting surface tractions on the vessel wall are important to analyze in order to understand various cardiovascular diseases (Formaggia et al., 2009).

Fluids and solids obey the fundamental conservation laws that hold for any adiabatic continuum body: the balance of linear and angular momentum and the conservation of mass. Without any consideration of a specific reference system, the balance of linear momentum and conservation of mass can be written in local form as

$$\begin{aligned} \mathrm{d}_t(\rho u) - \operatorname{div}\sigma &= b, && (40)\\ \mathrm{d}_t(\rho) &= 0. && (41) \end{aligned}$$

Equation (40) states the balance of linear momentum and equation (41) states the conservation of mass. Here, $\mathrm{d}_t(\cdot)$ denotes the total time derivative with respect to a given control volume, ρ denotes a density and u denotes a velocity. Moreover, σ denotes a stress tensor that is symmetric to satisfy the balance of angular momentum, and b a given body force per unit volume.

In an FSI problem, the fluid and the solid exchange and transfer data in terms of normal stresses (surface tractions) at a given common fluid-structure boundary. Denoting the fluid subproblem with a subscript F and the solid

subproblem with a subscript S, the following equilibrium equation holds for the surface tractions at the common fluid–structure interaction boundary:

$$\sigma_{_F} \cdot n_{_F} = -\sigma_{_S} \cdot n_{_S}, \tag{42}$$

where $n_{_F}$ and $n_{_S}$ denote the outward-pointing unit normal on the fluid–structure boundary, viewed from the fluid and structure domains, respectively. Hence, $n_{_F} = -n_{_S}$. The equilibrium equation (42) connects the conservation laws (40)-(41) for the different physics of the fluid subproblem and the structure subproblem. In addition to (42), we also require kinematic continuity at the boundary, that is, the velocity of the fluid and the solid are equal,

$$u_{_F} = u_{_S}. \tag{43}$$

Fluid and solid mechanics belong to the same branch of mechanics denoted continuum mechanics, so they obey the same conservation laws (see above). However, the constitutive behavior, i.e., the relationship between deformation (strains and strain rates) and the stress differ significantly. This fundamental difference requires different constitutive laws for modeling the fluid stress $\sigma_{_F}$ and the solid stress $\sigma_{_S}$. As a consequence, the kinematics for fluids and solids are naturally described in different frameworks.

These frameworks are referred to as the *Lagrangian framework* and the *Eulerian framework*. The kinematics of a solid is natural described in terms of the displacement in the Lagrangian framework (associated with the material domain) whereas a fluid is naturally described in terms of the velocity and pressure in the Eulerian framework (associated with the spatial domain).

In the remainder of this section, we will give an introduction to these different frameworks and explain how quantities may be transferred between the two frameworks. Moreover, we will also state the solid equations and the fluid equations governed by the constitutive laws for a St. Venant–Kirchhoff material and for an incompressible Newtonian fluid, respectively.

5.1 Lagrangian framework

The Lagrangian description of motion relates the motion of a body with respect to a fixed material coordinate X. In this description, attention is paid to each particle motion and one observes the labeled particles as they move through space. The position of a point is a function of the material coordinate X and the time t such that

$$x = \Phi(X, t). \tag{44}$$

A function $u(x,t)$ is referred to in the Lagrangian framework as $U(X,t) \equiv u(\Phi(X,t),t)$. We note that $\dot{X} = 0$ and the total time derivative in the Lagrangian framework is given by

$$\mathrm{D}_t(U(X,t)) = \dot{U}(X,t). \tag{45}$$

Thus, from the Lagrangian viewpoint, one observes the value at a material point X that moves with the velocity $U(X,t) = \dot{\Phi}$. The advantage with this framework is that the motion of individual particles is described and thus it serves as a natural framework for bodies that undergo moderate deformations over a relatively long period of time. Hence, the Lagrangian framework is a natural approach to model structural mechanics.

In conservative form, the balance of linear momentum and conservation of mass in the Lagrangian framework associated with the material domain Ω are given by

$$\frac{\mathrm{d}}{\mathrm{d}t}\int_\Omega \rho_0 U \,\mathrm{d}X = \int_{\partial\Omega} \Sigma \cdot N \,\mathrm{d}S + \int_\Omega B \,\mathrm{d}X, \tag{46}$$

$$\frac{\mathrm{d}}{\mathrm{d}t}\int_\Omega \rho_0 \,\mathrm{d}X = 0. \tag{47}$$

Here, ρ_0 is a reference density, U a velocity, Σ a stress tensor that is related to the symmetric Cauchy stress tensor as given below in (61), N a normal and B is a given body force per unit material volume. Equation (46) is Newton's second law stating that a material continuum is accelerated in proportion to the resulting forces acting on it. The conservation of mass (or the continuity equation) (47) states that mass can not be created, nor can it be destroyed. Recalling that the material domain Ω is fixed in space and using Gauss' theorem, we can formulate the corresponding local form:

$$\mathrm{D}_t(\rho_0 U) - \mathrm{Div}\,\Sigma = B, \tag{48}$$

$$\mathrm{D}_t(\rho_0) = 0. \tag{49}$$

We note that the total time derivative in the momentum equation is, by the continuity equation (49), $\mathrm{D}_t(\rho_0 U) = \rho_0 \dot{U}$.

5.2 Eulerian framework

The Eulerian framework relates the motion of a body with respect to the spatial point x at any given time t, where no attention is paid to each individual particle.

Each such spatial point x at time t corresponds to an initial material point X at time $t = 0$. Thus, the velocity in the Eulerian framework is interpreted as the velocity of the material point with the initial position X, i.e., $u(x,t) = \dot{x}$. The total time derivative of a function in the Eulerian framework is given by

$$\mathrm{d}_t(u) = \dot{u} + \operatorname{grad} u \cdot u. \tag{50}$$

The second term on the right-hand side is the convective rate of change and expresses the contribution of the particle motion (i.e., position change). In contrast to the Lagrangian framework, the Eulerian framework describes the behavior of a function at a specific spatial point instead of the behavior of each individual particle. This kind of description is thus a natural approach for modeling fluid flow since the movement of each individual particle in a fluid flow is less interesting than flow properties at certain spatial positions.

In conservative form, the balance of linear momentum and conservation of mass in the Eulerian framework associated with the spatial domain $\omega(t)$ are:

$$\int_{\omega(t)} (\dot{\rho u}) + \operatorname{div}(\rho u \otimes u)\,\mathrm{d}x = \int_{\partial\omega(t)} \sigma \cdot n\,\mathrm{d}s + \int_{\omega(t)} b\,\mathrm{d}x, \tag{51}$$

$$\int_{\omega(t)} \dot{\rho} + \operatorname{div}(\rho u)\,\mathrm{d}x = 0. \tag{52}$$

Here, ρ is a density, u a velocity, σ a (symmetric) stress tensor, n a normal, b is a given body force and $\otimes$ represents the tensor dyadic product, (i.e., $u \otimes u = u_i u_j$). The balance of linear momentum (51) is interpreted in the Eulerian framework as the net outflow from $\omega(t)$ that equals the resulting forces acting on it (minus the acceleration within $\omega(t)$). The corresponding interpretation of the continuity equation (52) is that the flux of matter into $\omega(t)$ must either exit or be accumulated within $\omega(t)$. Using Gauss theorem, we can write the local forms of (51) and (52) as

$$\begin{aligned} \mathrm{d}_t(\rho u) - \operatorname{div}\sigma &= b, & (53)\\ \dot{\rho} + \operatorname{div}(\rho u) &= 0. & (54) \end{aligned}$$

5.3 Transformation between frameworks

To be able to transform quantities from one framework to the other, the properties of the mapping Φ from equation (44) needs to be defined, where Φ describes the motion and deformation of the spatial domain $\omega(t)$ relative to the material domain Ω.

The motion of a body that undergoes deformation can be tracked by a sufficiently smooth bijective map Φ, parameterized by the common time coordinate $t \in [0, T]$. At any given time $t \in [0, T]$, $\Phi(X, t)$ maps the material point $X \in \Omega$ to its spatial position $x \in \omega(t)$ such that

$$\begin{aligned} \Phi(\cdot, t) : \Omega \quad &\rightarrow \quad \omega(t) = \Phi(\Omega, t), \quad t \in [0, T] \\ X \quad &\mapsto \quad x = \Phi(X, t), \quad X \in \Omega. \end{aligned} \tag{55}$$

Clearly, for $t = 0$ we have $\Omega = \omega(0)$. As mentioned earlier, for any function $U = U(X, t) \in \Omega$ there exists a corresponding function $u = u(x, t) \in \omega(t)$ defined by the composition of U with Φ, i.e.,

$$U(X, t) = u(\Phi(X, t), t), \quad X \in \Omega, \tag{56}$$

and we recall that the time derivative of the mapping defines the velocity relative to the reference domain such that $\dot{\Phi}(X, t) = \dot{x} = u(x, t)$. Thus, we relate the time derivatives in the reference domain of a function U with its counterpart u:

$$\mathrm{D}_t(U) = \mathrm{d}_t(u). \tag{57}$$

The non-singular Jacobian matrix of the mapping Φ is defined as

$$F = \mathrm{Grad}\, \Phi(X, t), \tag{58}$$

and the corresponding volume change is given by the Jacobian determinant $J = \det F$. To relate the stress tensor Σ with the stress tensor σ, we recall the Cauchy stress theorem (Gurtin, 1981) stating that there exist unique second order tensor fields $\sigma = \sigma(x, t)$ and $\Sigma = \Sigma(X, t)$ such that

$$\Sigma \cdot N = \sigma \cdot n, \tag{59}$$

where Σ and σ are the *first Piola stress* and the *Cauchy stress*, respectively. Using Nanson's formula, which relates boundary integrals such that

$$JF^{-\top} \cdot N \, \mathrm{d}(\partial\Omega) = n \, \mathrm{d}(\partial\omega(t)), \tag{60}$$

we can relate the Cauchy stress to the first Piola stress as

$$\Sigma = J\sigma \cdot F^{-\top}, \tag{61}$$

which is called the *Piola transform*. Thus the stresses are easily transformed from one framework to another.

5.4 Solid and fluid equations

Formulating the balance of linear momentum and conservation of mass is not sufficient to distinguish one solid material from another, or one fluid type from another. In addition, constitutive laws need to be specified for representing materials. Essentially, these constitutive laws are mathematical models that model the stress tensor as a function of a certain kinematic measures. In this section, we describe the set of constitutive laws that are used to model the structure (solid) equations and the fluid equations in this thesis, namely the St. Venant–Kirchhoff equations and the incompressible Navier–Stokes equations. For a more comprehensive treatment of constitutive laws for solids and continuum mechanics in general, see, e.g., Gurtin (1981); Holzapfel (2000) and for fluid mechanics, see, e.g., Panton (1984); Batchelor (1967); Welty et al. (2001).

5.4.1 The St. Venant–Kirchhoff equation

When formulating constitutive laws for the hyperelastic solid stress tensor Σ_S in the Lagrangian framework, it is natural to relate the stress to the *displacement field*. Deviating from the previously presented notation[2], the solid displacement field U_S associated with the Lagrangian solid domain $\Omega_S \times [0, T]$ is defined as

$$U_S(X, t) = \Phi_S(X, t) - X, \tag{62}$$

where we relate the deformation of the structure domain Ω_S with its corresponding mapping Φ_S, defined in the same manner as the mapping (55), for all $X \in \Omega_S$. The tangent map of the Lagrangian domain is given by the so-called deformation gradient tensor,

$$F_S = I + \operatorname{Grad} U_S, \tag{63}$$

where I denotes the identity matrix. A fundamental measure of a deforming body is the strain, which measures how much a given displacement differs locally from a rigid body displacement. One such strain measure is the Green–Lagrange strain tensor $E_S = \frac{1}{2}(F_S^\top F_S - I)$. Formulating constitutive laws for hyperelastic materials, the Frechét derivative of the strain energy functional $\Psi(E_S)$ can be related to the first Piola–Kirchhoff stress tensor Σ_S by

$$\Sigma_S = F_S \cdot \frac{\mathrm{d}\Psi(E_S)}{\mathrm{d}E_S}. \tag{64}$$

[2]This is motivated in order to get a consistent notation for the finite element formulation of adaptive FSI problems in Paper I and Paper III.

For the St. Venant–Kirchhoff model, which is a classical nonlinear model for a compressible elastic material with a constant reference density $\rho_{_S}$, the energy functional is defined as $\Psi(E_{_S}) = \mu_{_S}\ \mathrm{tr}(E_{_S}^2) + \frac{\lambda_{_S}}{2}(\mathrm{tr}(E))^2$, for some given positive Lamé constants $\mu_{_S}$ and $\lambda_{_S}$. Thus, we can formulate the strong form of the St. Venant–Kirchhoff equation in the Lagrangian framework as follow: find the displacement $U_{_S} : \Omega_{_S} \times [0,T] \to \mathbb{R}^d$ such that

$$\begin{aligned} \mathrm{D}_t^2(\rho_{_S} U_{_S}) - \mathrm{Div}\ \Sigma(U_{_S}) &= B_{_S} \qquad \text{in } \Omega_{_S} \times (0,T], \\ \mathrm{D}_t(\rho_{_S}) &= 0 \qquad \text{in } \Omega_{_S} \times (0,T], \end{aligned} \tag{65}$$

with corresponding initial and boundary conditions

$$\begin{aligned} U_{_S}(\cdot,0) &= U_{_S}^0 \qquad \text{in } \Omega_{_S}, \\ \dot{U}_{_S}(\cdot,0) &= U_{_S}^1 \qquad \text{in } \Omega_{_S}, \\ U_{_S} &= G_{_{S,D}} \qquad \text{on } \Gamma_{_D} \times (0,T], \\ \Sigma(U_{_S}) \cdot N_{_S} &= G_{_{S,N}} \qquad \text{on } \Gamma_{_N} \times (0,T]. \end{aligned} \tag{66}$$

Here, $B_{_S}$ is a given body force per unit reference volume and the acceleration term is given by $\mathrm{D}_t^2(\rho_{_S} U_{_S}) \equiv \rho_{_S} \ddot{U}_{_S}$, where $\rho_{_S}$ is the constant reference structure density. Since the reference density $\rho_{_S}$ is constant, the continuity equation is reduced to $\mathrm{D}_t(\rho_{_S}) = \dot{\rho}_{_S} = 0$ in the Lagrangian framework and thus we usually omit this equation in (65). The boundary $\partial\Omega$ is assumed to be divided into two parts $\Gamma_{_D}$ and $\Gamma_{_N}$ which are associated with the Dirichlet and Neumann conditions $G_{_{S,D}}$ and $G_{_{S,N}}$, respectively. In a coupled FSI problem, the Neumann boundary usually consists of at least one part which coincides with the fluid and defines the common fluid–structure interaction boundary $\Gamma_{_{FS}}$. Here, the traction force from the fluid is imposed as a Neumann condition. For a St. Venant–Kirchhoff material, the first Piola–Kirchhoff stress tensor $\Sigma_{_S}$ is given by

$$\Sigma_{_S}(U_{_S}) = F_{_S} \cdot (2\mu_{_S}\ E_{_S} + \lambda_{_S}\ \mathrm{tr}\,(E_{_S})I). \tag{67}$$

5.4.2 The incompressible Navier–Stokes equations

For fluids, the constitutive laws are essentially divided into two categories: Newtonian fluids and non-Newtonian fluids. The viscous stress of a Newtonian fluid is proportional to the rate of strain. For such fluids, the Cauchy stress tensor $\sigma_{_F}$ in the Eulerian framework is a function of the *fluid velocity* $u_{_F}(x,t)$ and the *fluid pressure* $p_{_F}(x,t)$ and it is given by

$$\sigma_{_F}(u_{_F}, p_{_F}) = 2\mu_{_F}\ \mathrm{grad}^{\mathbf{s}} u_{_F} - p_{_F} I. \tag{68}$$

Here, $2\mu_{_F}\ \mathrm{grad}^{\mathbf{s}} u_{_F} \equiv 2\mu_{_F}\ \frac{1}{2}(\mathrm{grad}\ u_{_F} + \mathrm{grad}\ u_{_F}^{\top})$ denotes the viscous stress tensor where $\mu_{_F}$ is the constant dynamic fluid viscosity. In addition, if we assume that the fluid is incompressible, we can formulate the strong form of Newtonian incompressible fluid flow, also know as the incompressible Navier–Stokes equations[3] in the Eulerian framework as follows: find the velocity $u_{_F} : \omega_{_F}(t) \to \mathbb{R}^d$ and the pressure $p_{_F} : \omega_{_F}(t) \to \mathbb{R}$ such that

$$\begin{aligned} \mathrm{d}_t(\rho_{_F} u_{_F}) - \mathrm{div}\ \sigma_{_F}(u_{_F}, p_{_F}) &= b_{_F} && \text{in } \omega(t), \\ \mathrm{div}\ u_{_F} &= 0 && \text{in } \omega(t), \end{aligned} \tag{69}$$

with the corresponding initial and boundary conditions

$$\begin{aligned} u_{_F}(\cdot, 0) &= u_{_F}^0 && \text{in } \omega_{_F}(0), \\ u_{_F} &= g_{_{F,D}} && \text{on } \gamma_{_{F,D}}(t), \\ \sigma_{_F}(u_{_F}, p_{_F}) \cdot n_{_F} &= g_{_{F,N}} && \text{on } \gamma_{_{F,N}}(t), \end{aligned} \tag{70}$$

for $0 < t \leq T$. Here, $b_{_F}$ is a given body force and the total time derivative is given by $\mathrm{d}_t(\rho_{_F} u_{_F}) = \rho_{_F}(\dot{u}_{_F} + \mathrm{grad}\ u_{_F} \cdot u_{_F})$ and $\rho_{_F}$ is the constant fluid density. The boundary $\partial\omega(t)$ is assumed to be divided into two parts $\gamma_{_D}$ and $\gamma_{_N}$, which are associated with the Dirichlet and Neumann conditions $g_{_{F,D}}$ and $g_{_{F,N}}$, respectively. In a coupled FSI problem, at least one part of the Dirichlet boundary coincides with the structure and defines the common fluid–structure boundary $\gamma_{_{FS}}(t)$, where the kinematic continuity from the structure problem is imposed.

6 Solving FSI problems

In the previous section, the governing continuous equations for the fluid (69) and the solid (65) were formulated in their natural frameworks. Via the mapping (55), it is possible to transfer traction forces from one framework to another and thus formulate an FSI problem. Typically, in a continuous formulation of an FSI problem, the stresses $\Sigma_{_S}$ and $\sigma_{_F}$ are transferred using the Piola transform (61) at the common fluid–structure boundary, denoted $\Gamma_{_{FS}}$ and $\gamma_{_{FS}}(t)$ in the Lagrangian and the Eulerian framework, respectively.

To combine the Lagrangian and the Eulerian frameworks in a *discrete finite element setting*, the deforming boundary $\gamma_{_{FS}}(t)$ needs to be tracked in the spatial

[3] The idea of the linear relation between stress and strain-rate was first proposed by Newton. Much later, Navier and Stokes produced the exact same equations that govern the flow for Newtonian fluid, hence the name Navier–Stokes.

fluid domain. The deformation of the boundary $\gamma_{FS}(t)$, given by the structure solution in the material domain, does not only influence the boundary conditions for the fluid; the mesh in the computational fluid domain must also be updated. A mesh obtained by simply moving the vertices at the fluid–structure interface, without any additional algorithms to enhance the mesh quality, will result in a very poor mesh quality. It is well known that poor quality meshes have a strong influence on the stability and accuracy of a numerical method. For this reason, an additional *mesh problem* has to be solved to enhance the mesh quality in the spatial fluid domain. This mesh problem can be formulated and solved in various ways, see, e.g., Hermansson and Hansbo (2003); López et al. (2008); Hansbo (1995). However, rearranging the vertices to avoid mesh distortion will result in an additional movement (excluding the vertices attached to the boundary $\gamma_{FS}(t)$) of the fluid problem in the spatial domain and this movement needs to be accounted for in the FSI algorithm. A common numerical technique to handle this is the so-called *Arbitrary Lagrangian–Eulerian* (ALE) formulation of the FSI problem; see Donea et al. (2004); Hughes et al. (1981); Donea et al. (1982). In the subsequent section, we explain briefly the ALE method for solving FSI problems.

6.1 The ALE formulation of an FSI problem

As a result of introducing an additional mesh problem, an arbitrary framework of reference is needed which is independent of both the Lagrangian and the Eulerian description. This arbitrary reference domain is often the initial computational domain which typically is undeformed.

For the sake of simplicity, we now let $\Omega \subset \mathbb{R}^d$ $(d = 2, 3)$, denote the *reference* computational domain at time $t = 0$. Further, we let Ω be partitioned into two disjoint subsets Ω_F, the fluid domain, and Ω_S, the structure (solid) domain. Moreover, we let $\omega(t)$, ω_F and ω_S denote the corresponding *current* computational domains.

6.1.1 Domain mappings

In order to map quantities from the current computational domain $\omega(t)$ and the reference computational domain Ω, we now let Φ denote the sufficiently smooth bijective "ALE map" $\Phi(\cdot, t) : \Omega \to \omega(t)$. At any fixed time $t \in [0, T]$, $\Phi(\cdot, t)$ maps a reference point $X \in \Omega$ to a corresponding current point $x \in \omega(t)$:

$$X \mapsto x = \Phi(X, t). \tag{71}$$

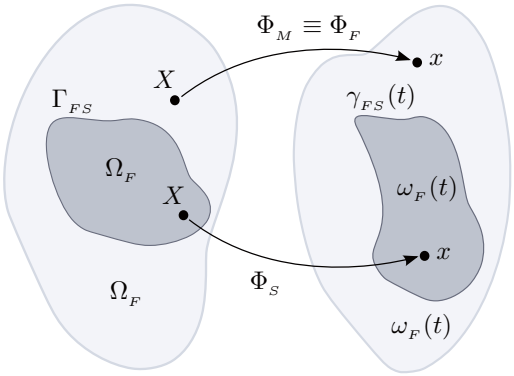

Figure 2: The reference computational domain Ω and the current computational domain $\omega(t)$. A reference point X maps to the current point x via the ALE mapping $\Phi(X,t)$. Since we allow the meshes to deform independently, the ALE map is split into two parts: Φ_S and Φ_M, which are associated with structure subdomain and the fluid subdomain, respectively.

As a consequence of introducing the mesh problem in the current fluid domain $\omega_F(t)$, we allow the fluid and structure portions of the domain to deform independently, only enforcing that these deformations are identical on the common boundary, $\gamma_{FS}(t)$, and we split the map Φ as follows:

$$\Phi(X,t) = \begin{cases} \Phi_S(X,t), & X \in \Omega_S,\ 0 \le t \le T, \\ \Phi_M(X,t), & X \in \Omega_F,\ 0 \le t \le T. \end{cases} \tag{72}$$

Here, Φ_S is the map introduced in (62) and thus describes the (physical) deformation of the structure computational domain. The additive map Φ_M is defined as

$$\Phi_M(X,t) = X + U_M(X,t), \tag{73}$$

where U_M is the solution (displacement field) to an arbitrarily chosen mesh problem. The mesh problem can be solved in either the current domain or the reference domain and then pushed forward to the current domain. For convenience, we choose the latter and we choose the following mesh problem:

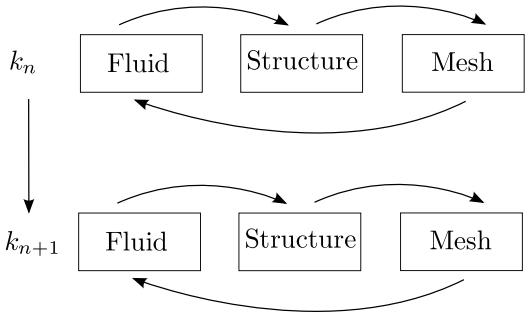

Figure 3: A partitioned FSI algorithm. In each time step k_n, the three subproblems are solved iteratively using a simple fixed point method.

find the mesh displacement $U_{\scriptscriptstyle M} : \Omega_{\scriptscriptstyle F} \times [0,T] \to \mathbb{R}^d$ such that

$$\begin{aligned} \dot{U}_{\scriptscriptstyle M} + \mathrm{Div}\, \Sigma_{\scriptscriptstyle M}(U_{\scriptscriptstyle M}) &= 0 \qquad && \text{in } \Omega_{\scriptscriptstyle F} \times (0,T], \\ U_{\scriptscriptstyle M}(\cdot,0) &= 0 \qquad && \text{in } \Omega_{\scriptscriptstyle F}, \\ U_{\scriptscriptstyle M} &= U_{\scriptscriptstyle S} \qquad && \text{on } \Gamma_{\scriptscriptstyle FS} \times (0,T]. \end{aligned} \tag{74}$$

In (74), the "mesh stress tensor" $\Sigma_{\scriptscriptstyle S}$ is defined in a similar way as for linear elasticity:

$$\Sigma_{\scriptscriptstyle M}(U_{\scriptscriptstyle M}) = 2\mu_{\scriptscriptstyle M}\, \mathrm{Grad}^{\mathbf{s}} U_{\scriptscriptstyle M} + \lambda_{\scriptscriptstyle M} \mathrm{tr}(\mathrm{Grad}\, U_{\scriptscriptstyle M}) I, \tag{75}$$

for some positive constants $\mu_{\scriptscriptstyle M}$ and $\lambda_{\scriptscriptstyle M}$. As input data for the mesh problem (74), the solid displacement $U_{\scriptscriptstyle S}$ is set as a Dirichlet condition at the common fluid–structure boundary $\Gamma_{\scriptscriptstyle FS}$.

6.1.2 Algorithmic considerations

A straightforward approach to solving the coupled FSI system consisting of the three subproblems for the fluid, the solid and the mesh is to use an iterative method. In such a partitioned algorithm, the three subproblems are solved using a simple fixed point iteration in each time step as depicted in Figure 3.

To couple the three subproblems, we impose the following boundary conditions at the common fluid–structure boundaries $\Gamma_{\scriptscriptstyle FS}$ and $\gamma_{\scriptscriptstyle FS}(t)$:

$$(J_{\scriptscriptstyle M} \sigma_{\scriptscriptstyle F}(\Phi_{\scriptscriptstyle M}) \cdot F_{\scriptscriptstyle M}^{-\top}) \cdot N = \Sigma_{\scriptscriptstyle S} \cdot N, \tag{76}$$

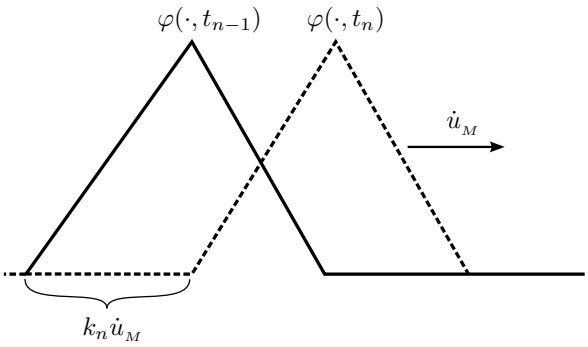

Figure 4: A sketch illustrating a moving Lagrange basis function in 1D in the moving fluid domain $\omega_{F}(t)$. The velocity of the basis function is given by the mesh velocity $\dot{u}_{M}$. The basis function φ^{n-1} at time $t = t_{n-1}$ is moved the distance $k_n \dot{u}_{M}$ to reach the position where the basis function φ^{n} is defined for $t = t_n$.

$$u_{F} = \dot{u}_{S}, \tag{77}$$

$$U_{M} = U_{S}, \tag{78}$$

where $F_{M} \equiv I + \text{Grad } U_{M}$ and $J_{M} \equiv \det F_{M}$. The boundary conditions (76)-(77) account for equilibrium of traction forces and for the kinematic continuity, and (78) makes sure that the fluid and structure subdomains coincide on the common interface.

To account for the additional (unphysical) mesh movement introduced by the mesh problem (74), the mesh displacement U_{M} is pushed forward to the current fluid domain $\omega_{F}(t)$ where $\dot{u}_{M}$ represents the current *mesh velocity*. This mesh velocity affects the basis functions on the fluid domain $\omega_{F}(t)$, depicted in Figure 4. By construction, $\varphi(x,t) = \varphi^{n}(x - (t - t_{n-1})\dot{u}_{M}, t_{n-1})$ and by the chain rule, we obtain the time derivative of the moving basis function as $\dot{\varphi} = -\text{grad}\,\varphi \cdot \dot{u}_{M}$. To compensate for this extra mesh movement, an additional (negative) convective mesh velocity term appears in the discrete finite element formulation in the fluid momentum equation; see Paper I and Paper III for details.

With the proposed algorithm, the three subproblems can be solved individually, allowing the different problems to be solved using different numerical methods. This is advantageous, since the different physics of the fluid and the structure require different types of methods. Thus, for each subproblem, we

can use specific numerical methods that are optimized to solve each given subproblem. In short, we have chosen to solve the subproblems using the following methods:

- Fluid subproblem: Incremental Pressure Correction Scheme (IPCS) by Goda (1979);
- Structure subproblem: A standard cG(1)cG(1) method (Eriksson et al., 1996) solved on each time step with Newton's method;
- Mesh subproblem: A standard cG(1)cG(1) method.

For a more comprehensive discussion on the above methods, as well as the iterative method used to solve the coupled FSI problem, see Paper I and Paper III. Moreover, for a discussion on the IPCS method, see Paper II.

The presented method for handling the coupling between the subproblems is one of the most basic algorithms. Another approach is the Immersed Boundary (IB) method by Peskin (2002) which employs a mixture of Eulerian and Lagrangian variables. The IB method uses an *a priori* fixed mesh on which the fluid and structure equations are solved simultaneously. The interaction of the fluid and structure is handle by an interaction equation where the Dirac delta function plays a prominent role. In the IB formulation, the Eulerian variables are defined on a fixed Cartesian mesh and the Lagrangian variables are defined on a curved linear mesh that moves freely through the fixed Cartesian mesh.

The Fictitious Domain (FD) method by Diniz dos Santos et al. (2008), originally designed for rigid particles on fixed meshes, considers independent meshes for the fluid and the structure. By enforcing a kinematic condition with Lagrange multipliers, the interaction between the fluid and the structure is obtained.

Another approach that uses Lagrange multipliers for FSI problems is the eXtended Finite Element Method (XFEM) by Gerstenberger and Wall (2008). In this method, the extended Eulerian fluid field and the Lagrangian structure field are partitioned and iteratively coupled using a Lagrange multiplier technique.

7 Goal-oriented FEM for FSI

Numerical simulations of FSI problems in general require large computational resources, and it is typically the fluid subproblem that requires the most computational resources in the coupled system; see, e.g., Farhat (2004). As for all numerical simulations, regardless of application, the computational cost of

the solution and the accuracy reached for a given cost are important issues. On many occasions, the goal is not to resolve the system in full detail throughout the entire space–time domain; instead the analysis and quantification of a specific target functional is of more interest. As an example, when simulating vascular FSI problems, quantities of hemodynamic interest such as the wall shear stress and wall tension are common target functionals (Bazilevs et al., 2010). Thus, goal-oriented adaptive finite element methods are highly relevant for studying FSI problems.

7.1 Earlier work

During the last decade, research on goal-oriented adaptive finite element methods for FSI has emerged. One of the first works in this field was published by Grätsch and Bathe (2006), who analyzed two different sets of stationary FSI problems. This paper studies the sharpness of error estimates obtained by a dual-weighted residual method but no adaptive method is considered. The study presents very good quality efficiency indices for the FSI problem.

Based on a full monolithic formulation in both the Eulerian and the ALE frameworks, Dunne (2007) developed a dual-weighted residual method for a two-way coupled FSI problem. In this method, the different physics of the fluid and the structure are tracked using a so-called initial positions set method. The presented numerical results are for both stationary and time-dependent problems. However, the adaptivity in both the stationary and time-dependent cases are based on adaptive h-refinement (the selection of time steps is based on a fractional time stepping scheme). Good quality efficiency indices are presented for a stationary fluid problem governed by a Stokes flow and a nonlinear structure. The method has been further refined and discussed in Dunne and Rannacher (2006); Dunne (2006); Bönisch et al. (2008).

In the work by van der Zee et al. (2008); van der Zee (2009); van der Zee et al. (2010a), FSI problems of free boundary character are studied. The presented numerical results consider Stokes flow with an elastic part of the boundary represented by a low-order structural (string) model. By using a domain map linearization approach, the corresponding linearized dual is derived with respect to the domain geometry. The adaptivity relies upon adaptive h-refinement and the method is applied on different sets of problems. Good quality efficiency indices are presented.

In Fick et al. (2010), an adaptive finite element method is presented for a time-dependent FSI problem. Here, the fluid subproblem is assumed to be governed by a simplified inviscid fluid and the structure kinematics is modeled by an

Euler–Bernoulli beam. The FSI problem is analyzed using a so-called adjoint-consistent formulation and adaptive methods for h- and hp-refinement are considered. The numerical results, in particular for the adaptive hp-refinement, demonstrate very good efficiency indices.

In Bengzon and Larson (2010), the authors develop an adaptive finite element method for a one-way coupled stationary FSI problem. In this paper, the fluid is governed by a Stokes flow and the structure is modeled using linear elasticity. The adaptivity is based on adaptive h-refinement. The authors do not present any results regarding efficiency indices.

7.2 Contributions of this thesis

In Paper I and Paper III, we develop a goal-oriented time-dependent adaptive finite element method using a dual-weighted residual method for fully coupled FSI problems. The fluid subproblem is modeled by the incompressible Navier–Stokes equations and the movement of the fluid domain is handled using an ALE method. The structure subproblem is modeled using a nonlinear hyperelastic model (St. Venant–Kirchhoff) and the movement of the mesh is modeled using a linear (time-dependent) elasticity problem. By relating the three subproblems on a fixed reference mesh, we derive a linearized dual problem and a corresponding *a posteriori* error estimate for the fully coupled, time-dependent FSI problem. The error estimate captures errors resulting from space discretization, time discretization and the use of an inconsistent operator splitting method. The adaptivity is based on adaptive h-refinement and adaptive time-stepping.

In the remainder of this section, we briefly explain the methodology of our developed adaptive finite element method for FSI problems. This methodology relies on the principles of adaptivity described in Section 3 and the presented FSI formulation in Section 6. For the sake of clarity, the presentation is kept simple and abstract. All details, and in particular the full dual problem, are presented in Paper I. For a discussion of the implementation of the proposed methodology in practice, we refer to Paper III.

Let (f) denote the fluid subproblem (69) defined on the current fluid domain $\omega_{_F}(t)$ and let (S) denote the structure subproblem (65) defined on the reference structure domain $\Omega_{_S}$. Further, let (M) denote the mesh subproblem (74) defined on the reference fluid domain $\Omega_{_F}$. We thus obtain the partitioned FSI problem (f, S, M),

The strong primal coupled problem (f, S, M) is assumed to be solved using the presented partitioned algorithm described in Section 6.1.2. In this algorithm, we use an inconsistent splitting method to solve the fluid subproblem and a pure

Galerkin method for the structure and the mesh subproblems. Let this discrete problem be denoted $(d(f)^\bigstar, d(S), d(M))$, were d indicates that it is a discrete numerical solution and $\bigstar$ emphasizes that the fluid subproblem is solved using an inconsistent (non-Galerkin) method. In order to formulate a continuous dual problem for the error analysis of $(d(f)^\bigstar, d(S), d(M))$, we need to handle two fundamental challenges:

i) The fluid subproblem $d(f)^\bigstar$ is solved using a non-Galerkin method.

ii) The coupled problem $(d(f)^\bigstar, d(S), d(M))$ is solved in different domains with different reference frameworks.

The first challenge may be handled by including in the analysis the effect of computational errors η_c accounting for the fact that the Galerkin orthogonality is not satisfied, as was demonstrated in Section 3. This is investigated in more detail for the fluid subproblem in Paper II.

The methodology for the error analysis of coupled problems developed in Section 4 assumes that all subsystems are formulated on the same (fixed) domain, which is not the case for the primal system (f, S, M). We therefore use the map $\Phi_{_M}^{-1}$ to pull back the fluid subproblem (f) to the reference fluid domain $\Omega_{_F}$, where a corresponding fluid subproblem (F) is formulated. One may then directly apply the machinery presented in Section 4 to derive the dual problem of the fully coupled problem (F, S, M) posed on the reference domain. In particular, we derive the corresponding weak problem $(w(F), w(S), w(M))$, from which the weak dual problem $(w(F), w(S), w(M))^*$ follows by linearization. The resulting weak dual problem is a system of six time-dependent, linear and coupled partial differential equations. Although the dual problem is quite complex, spanning more than a full page in very compact notation, its derivation is completely mechanical and relies on repeated use of the chain rule and other well known differentiation rules. The use of a modern programming environment (FEniCS/DOLFIN) also helps, since it allows the dual problem to be implemented in near identical notation to its mathematical formulation. An overview of the various subproblems involved in the analysis is given in (79) below.

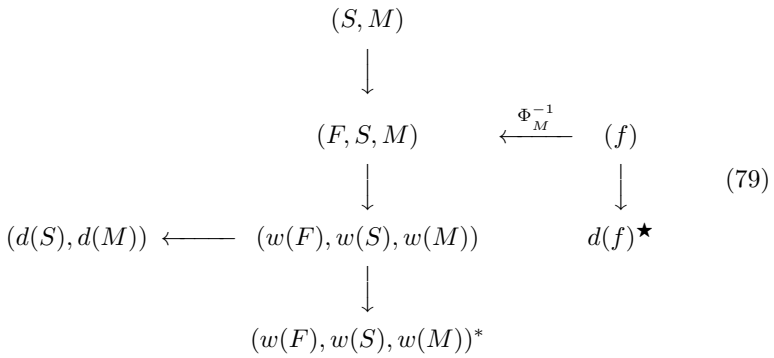

(79)

References

I. Babuška and W. W. C. Rheinboldt. A posteriori error estimates for the finite element method. *International Journal for Numerical Methods in Engineering*, 12(10):1597–1615, 1978. ISSN 1097-0207.

W. Bangerth and R. Rannacher. *Adaptive finite element methods for differential equations*. Birkhäuser, 2003.

G. Batchelor. *An introduction to fluid dynamics*. Cambridge Univ Pr, 1967.

Y. Bazilevs, M. Hsu, Y. Zhang, W. Wang, T. Kvamsdal, S. Hentschel, and J. Isaksen. Computational vascular fluid–structure interaction: Methodology and application to cerebral aneurysms. *Biomechanics and modeling in mechanobiology*, pages 1–18, 2010. ISSN 1617-7959.

R. Becker and R. Rannacher. Weighted a posteriori error control in finite element methods. *preprint*, pages 96–1, 1995.

R. Becker and R. Rannacher. A feed-back approach to error control in finite element methods: Basic analysis and examples. *East West Journal of Numerical Mathematics*, 4:237–264, 1996.

R. Becker and R. Rannacher. An optimal control approach to a posteriori error estimation in finite element methods. *Acta Numerica 2001*, 10:1–102, 2001.

R. Becker, V. Heuveline, and R. Rannacher. An optimal control approach to adaptivity in computational fluid mechanics. *International Journal for Numerical Methods in Fluids*, 40(1-2):105–120, 2002.

F. Bengzon and M. G. Larson. Adaptive finite element approximation of multiphysics problems: A fluid–structure interaction model problem. *International Journal for Numerical Methods in Engineering*, 2010.

S. Bönisch, T. Dunne, and R. Rannacher. Numerics of fluid–structure interaction. *Hemodynamical Flows*, pages 333–378, 2008.

S. C. Brenner and L. R. Scott. *The Mathematical Theory of Finite Element Methods*, volume 15 of *Texts in Applied Mathematics*. Springer, New York, third edition, 2008. URL `http://dx.doi.org/10.1007/978-0-387-75934-0`.

R. Clough. The finite element method in plane stress analysis. *Proceedings of 2nd ASCE Conference on Electronic Computation, Pittsburgh, PA*, pages 8–9, 1960.

R. Courant. Variational methods for the solution of problems of equilibrium and vibrations. *Bull. Am. Math. Soc.*, 49:1–23, 1943.

L. Debnath and P. Mikusiński. *Introduction to Hilbert spaces with applications*. Academic Pr, 1999.

N. Diniz dos Santos, J. Gerbeau, and J. Bourgat. A partitioned fluid–structure algorithm for elastic thin valves with contact. *Computer Methods in Applied Mechanics and Engineering*, 197(19-20):1750–1761, 2008.

J. Donea, S. Giuliani, and J. Halleux. An arbitrary Lagrangian–Eulerian finite element method for transient dynamic fluid–structure interactions. *Computer Methods in Applied Mechanics and Engineering*, 33(1-3):689–723, 1982.

J. Donea, A. Huerta, J. Ponthot, and A. Rodrıguez-Ferran. Arbitrary Lagrangian–Eulerian methods. *Encyclopedia of Computational Mechanics*, 1:1–25, 2004.

W. Dörfler. A convergent adaptive algorithm for Poisson's equation. *SIAM Journal on Numerical Analysis*, 33(3):1106–1124, 1996.

T. Dunne. An Eulerian approach to fluid–structure interaction and goal-oriented mesh adaptation. *International Journal for Numerical Methods in Fluids*, 51 (9-10):1017–1039, 2006.

T. Dunne. *Adaptive Finite Element Approximation of Fluid–Structure Interaction Based on Eulerian and Arbitrary Lagrangian-Eulerian Variational Formulations*. PhD thesis, Ruprecht-Karls-Universität, Heidelberg, 2007.

T. Dunne and R. Rannacher. Adaptive finite element approximation of fluid–structure interaction based on an Eulerian variational formulation. *Fluid–structure interaction*, pages 110–145, 2006.

K. Eriksson and C. Johnson. Adaptive finite element methods for parabolic problems I: A linear model problem. *SIAM Journal on Numerical Analysis*, pages 43–77, 1991.

K. Eriksson and C. Johnson. Adaptive finite element methods for parabolic problems IV: Nonlinear problems. *SIAM Journal on Numerical Analysis*, 32 (6):1729–1749, 1995.

K. Eriksson, D. Estep, P. Hansbo, and C. Johnson. Introduction to adaptive methods for differential equations. *Acta numerica*, 4:105–158, 1995.

K. Eriksson, D. Estep, P. Hansbo, and C. Johnson. *Computational Differential Equations*. Cambridge Univ Pr, 1996. ISBN 0521567386.

D. Estep. A posteriori error bounds and global error control for approximations of ordinary differential equations. *SIAM J. Numer. Anal.*, 32:1–48, 1995.

D. Estep and D. French. Global error control for the continuous Galerkin finite element method for ordinary differential equations. *RAIRO-M2AN Modelisation Math et Analyse Numerique-Mathem Modell Numerical Analysis*, 28(7): 815–852, 1994.

D. Estep, M. Larson, and R. Williams. Estimating the error of numerical solutions of systems of nonlinear reaction–diffusion equations. *Memoirs of the American Mathematical Society*, 696:1–109, 2000.

C. Farhat. CFD-based nonlinear computational aeroelasticity. *Encyclopedia of computational mechanics*, 3:459–480, 2004.

P. W. Fick, E. H. van Brummelen, and K. G. van der Zee. On the adjoint-consistent formulation of interface conditions in goal-oriented error estimation and adaptivity for fluid-structure interaction. *Computer Methods in Applied Mechanics and Engineering*, 2010. ISSN 0045-7825.

L. Formaggia, A. Quarteroni, and A. Veneziani. *Cardiovascular mathematics: Modeling and simulation of the circulatory system*, volume 1. 2009.

G. Foufas. *Valuing Path-Dependent Options using the Finite Element Method, Duality Techniques, and Model Reduction*. PhD thesis, Chalmers University of Technology and University of Göteborg, 2008.

B. Galerkin. Series solution of some problems in elastic equilibrium of rods and plates. *Vestnik inzhenerov i tekhnikov*, 19(7):897–908, 1915.

A. Gerstenberger and W. Wall. An extended finite element method/Lagrange multiplier based approach for fluid–structure interaction. *Computer Methods in Applied Mechanics and Engineering*, 197(19-20):1699–1714, 2008.

K. Goda. A multistep technique with implicit difference schemes for calculating two-or three-dimensional cavity flows. *Journal of Computational Physics*, 30 (1):76–95, 1979. ISSN 0021-9991.

T. Grätsch and K. Bathe. Goal-oriented error estimation in the analysis of fluid flows with structural interactions. *Computer Methods in Applied Mechanics and Engineering*, 195(41-43):5673–5684, 2006.

M. Gurtin. *An introduction to continuum mechanics*. Academic Pr, 1981.

P. Hansbo. Generalized Laplacian smoothing of unstructured grids. *Communications in Numerical Methods in Engineering*, 11(5):455–464, 1995.

J. Hermansson and P. Hansbo. A variable diffusion method for mesh smoothing. *Communications in Numerical Methods in Engineering*, 19(11):897–908, 2003.

V. Heuveline and R. Rannacher. A posteriori error control for finite element approximations of elliptic eigenvalue problems. *Advances in Computational Mathematics*, 15(1):107–138, 2001. ISSN 1019-7168.

J. Hoffman. On duality based a posteriori error estimation in various norms and linear functionals for LES. *SIAM J. Sci. Comput*, 26(1):178–195, 2004.

G. Holzapfel. *Nonlinear solid mechanics*. John Wiley & Sons Inc, 2000.

T. Hughes, W. Liu, and T. Zimmermann. Lagrangian–Eulerian finite element formulation for incompressible viscous flows. *Computer methods in applied mechanics and engineering*, 29(3):329–349, 1981.

J. P. De S. R. Gago, D. W. Kelly, O. C. Zienkiewicz, and I. Babuska. A posteriori error analysis and adaptive processes in the finite element method: Part ii – Adaptive mesh refinement. *International Journal for Numerical Methods in Engineering*, 19(11):1621–1656, 1983. ISSN 1097-0207.

D. W. Kelly, J. P. De S. R. Gago, O. Zienkiewicz, and I. Babuška. A posteriori error analysis and adaptive processes in the finite element method: Part I - error analysis. *International Journal for Numerical Methods in Engineering*, 19(11):1593–1619, 1983. ISSN 1097-0207.

E. Kreyszig. *Introductory Functional Analysis with Applications*. John Wiley & Sons Inc, 1978.

M. Larson and F. Bengzon. Adaptive finite element approximation of multiphysics problems. *Communications in Numerical Methods in Engineering*, 24 (6):505–521, 2008.

M. Larson and A. Målqvist. Goal oriented adaptivity for coupled flow and transport problems with applications in oil reservoir simulations. *Computer Methods in Applied Mechanics and Engineering*, 196(37-40):3546–3561, 2007.

A. Logg. Multi-adaptive Galerkin methods for ODEs I. *SIAM J. Sci. Comput.*, 24(6):1879–1902, 2003. ISSN 1064-8275.

A. Logg. *Automation of computational mathematical modeling*. PhD thesis, Chalmers University of Technology and University of Göteborg, 2004.

A. Logg and G. N. Wells. DOLFIN: Automated finite element computing. *ACM Transactions on Mathematical Software*, 32(2):1–28, 2010.

E. López, N. Nigro, and M. Storti. Simultaneous untangling and smoothing of moving grids. *International Journal for Numerical Methods in Engineering*, 76(7):994–1019, 2008.

J. Nitsche. Über ein Variationsprinzip zur Lösung von Dirichlet-Problemen bei Vermendung von Teilrämen, die keinen Randbedingungen unterworfen sind. *Abh. Math. Sem. Univ. Hamburg*, 11:9–15, 1971.

J. Oden and L. Demkowicz. *Applied functional analysis*. CRC, 1996.

R. Panton. *Incompressible flow*. John Wiley & Sons Inc, 1984.

C. Peskin. The immersed boundary method. *Acta Numerica*, 11:479–517, 2002. ISSN 0962-4929.

R. Rannacher and F. Suttmeier. A posteriori error control in finite element methods via duality techniques: Application to perfect plasticity. *Computational mechanics*, 21(2):123–133, 1998. ISSN 0178-7675.

W. Ritz. Über eine neue Methode zur Lösung gewisser Variationsprobleme der mathematischen Physik. *Journal für die reine und angewandte Mathematik (Crelle's Journal)*, 1909(135):1–61, 1909.

M. Rognes and A. Logg. Automated goal-oriented error control I: Stationary variational problems. *SIAM Journal on Scientific Computing (in review)*, 2010.

R. Sandboge. Adaptive finite element methods for reactive compressible flow. *Mathematical Models and Methods in Applied Sciences*, 9(2):211–242, 1999. ISSN 0218-2025.

M. Turner, R. Clough, H. Martin, and L. Topp. Stiffness and deflection analysis of complex structures. *J. Aero. Sci*, 23(9):805–823, 1956.

K. G. van der Zee. *Goal-Adaptive Discretization of Fluid–Structure Interaction*. PhD thesis, Technische Universiteit Delft, 2009.

K. G. van der Zee, E. H. van Brummelen, and R. de Borst. Goal-oriented error estimation for Stokes flow interacting with a flexible channel. *International Journal for Numerical Methods in Fluids*, 56(8):1551–1557, 2008.

K. G. van der Zee, E. H. van Brummelen, I. Akkermanc, and R. de Borstd. Goal-oriented error estimation and adaptivity for fluid–structure interaction using exact linearized adjoints. *Comput. Methods Appl. Mech. Engrg.*, 2010a.

K. G. van der Zee, E. H. van Brummelen, and R. de Borst. Goal-oriented error estimation and adaptivity for free-boundary problems: The domain-map linearization approach. *SIAM J. Sci. Comput*, 32:1064–1092, 2010b.

K. G. van der Zee, E. H. Van Brummelen, and R. De Borst. Goal-oriented error estimation and adaptivity for free-boundary problems: The shape linearization approach. *SIAM J. Sci. Comput*, 32(2):1093–1118, 2010c.

J. Welty, C. Wicks, and R. Wilson. *Fundamentals of momentum, heat, and mass transfer*. John Wiley & Sons Inc, 2001.

Paper I

An Adaptive Finite Element Method for Fluid–Structure Interaction

Paper II

An Adaptive Finite Element Splitting Method for the Incompressible Navier–Stokes Equations

Paper III

An Adaptive Finite Element Solver for Fluid–Structure Interaction Problems